COMPUTER SIMULATION OF STRUCTURAL TRANSFORMATIONS DURING PRECIPITATION OF AN ORDERED INTERMETALLIC PHASE

LONG-QING CHEN and A. G. KHACHATURYAN

Department of Mechanics and Materials Science, Rutgers University, P.O. Box 909,
Piscataway, NJ 08855, U.S.A.

Abstract---A computer simulation of the kinetics of precipitation of an ordered intermetallic phase from a disordered solid solution in a model binary two-dimensional alloy is considered. All diffusion processes, the concentrational delamination (clustering), ordering, antiphase domain boundary movement and coarsening, are described by the microscopic kinetic equations. The ordering transition of the first and second kinds are considered. It is shown that the conventional precipitation mechanism through nucleation and growth of an equilibrium ordered phase occurs only in a very narrow "strip" of the two-phase field in the phase diagram. In the remaining part, the decomposition always starts from a congruent ordering, which produces a transient nonstoichiometric ordered single-phase state with the same composition as the parent disordered phase and the same symmetry as the product intermetallic phase. Decomposition of the transient ordered phase occurs predominantly at the antiphase domain boundaries (APBs), which results in a two-phase morphology with layers of disordered films separating antiphase domains of the ordered phase. This decomposition is a result of a concentration instability on APBs, which is more substantial than the conventional homogeneous spinodal instability. Further morphological evolution after decomposition is controlled by coarsening, which reduces the order/disorder interfacial area. The predicted precipitation mechanism through a formation of a single-phase transient ordered state is general. It is expected in the most part of a two-phase field of a phase diagram of any alloy systems with intermetallic precipitates related to the parent one by ordering.

Résumé—On considère une simulation par ordinateur de la cinétique de précipitation d'une phase ordonnée intermétallique à partir d'une solution solide désordonnée dans un modèle d'alliage binaire à deux dimensions. Tous les processus de diffusion, la délamination de concentration (formation d'amas), l'ordre, le mouvement de parois d'antiphase et le grossissement des domaines sont décrits par des équations cinétiques microscopiques. Les transitions d'ordre du premier et du second ordre sont considérées. On montre que le mécanisme habituel de précipitation par germination et croissance d'une phase ordonnée en équilibre se produit dans une très étroite "bande" du domaine biphasé du le diagramme d'équilibre. Dans la partie restante, la décomposition part toujours de l'ordre congruent qui produit un état transitoire de phase unique ordonnée non stoechiométrique de même composition que la phase mère désordonnée et de même symétrie que la phase intermétallique produite. La décomposition de la phase transitoire ordonnée a lieu préférentiellement sur les parois d'antiphase (PAP), ce qui produit une morphologie à deux phases avec des couches de films désordonnés séparant des domaines d'antiphase de la phase ordonnée. Cette décomposition est le résultat de l'instabilité de la concentration sur les PAP, instabilité qui est plus importante que celle correspondant à la transformation spinodale homogène classique. Une évolution morphologique ultérieure après la décomposition est contrôlée par le grossissement qui réduit la surface de l'interface ordre-désordre. Le mécanisme de précipitation prévu qui s'opère par la formation d'un état ordonné transitoire monophasé est général. Il est attendu dans la plus grande partie du domaine biphasé du diagramme d'équilibre d'un alliage quelconque ayant des précipités intermétalliques liés à la matrice par la mise en ordre.

Zusammenfassung—Die Kinetik der Ausscheidung einer geordneten intermetallischen Phase aus einem entordneten Mischkristall wird in einer binären zweidimensionalen Modell-Legierung mit dem Rechner simuliert. Sämtliche Diffusionsprozesse, die konzentrationsmäßige Ablösung (Clusterbildung), die Ordnungseinstellung, die Bewegung der Antiphasengrenzen und die Vergröberung werden mit mikroskopischen Kinetik-Gleichungen beschrieben. Die Ordnungsübergänge erster und zweiter Art werden berücksichtigt. Es wird gezeigt, daß die konventionelle Ausscheidung über Keimbildung und Wachstum einer geordneten Gleichgewichtsphase nur in einem sehr engen "Streifen" im Zweiphasenfeld des Phasendiagrammes auftritt. Im übrigen Bereich beginnt die Entwicklung mit einer kongruenten Ordnungseinstellung, welche übergangsweise einen nicht-stöchiometrischen geordneten einphasigen Zustand mit derselben Zusammensetzung wie die entordnete Mutterphase und derselben Symmetrie wie die intermetallische Produktphase erzeugt. Der Zerfall dieser Phase läuft überwiegend an den Antiphasengrenzen ab, welches zu einer zweiphasigen Morphologie führt mit Schichten aus entordneten Filmen, die die Antiphasenbereiche der geordneten Phase trennen. Der Zerfall rührt her von einer Konzentrationsinstabilität an den Antiphasengrenzen, welche bedeutender ist als die konventionelle homogene spinodale Instabilität ist. Die weitere morphologische Entwicklung nach dem Zerfall wird gesteuert durch die Vergröberung, welche die Gesamtfläche der Ordnungs-/Entordnungs-Grenzen verringert. Dieser vorausgesagte Ausscheidungsmechanismus durch Bildung eines einphasigen Übergangs-Ordnungszustandes gilt allgemein. Er wird im überwiegenden Teil eines zweiphasigen Feldes eines Phasendiagrammes einer jeden Legierung mit intermetallischen Ausscheidungen, die mit der Mutterphase über Ordnungseinstellung verwandt sind, erwartet.

1. INTRODUCTION

The problem of structural transformations during the alloy aging is of paramount importance for the materials design of advanced engineering materials since different structural states, formed along the transformation path, are utilized for achieving special properties. Very often the decomposition of a homogeneous parent phase produces two effects, the concentrational delamination due to atomic diffusion and the crystal lattice symmetry changes associated with the composition change. The crystal symmetry changes may occur due to either ordering or a crystal lattice rearrangement. In both cases the composition alone is not sufficient to describe all possible phase states and a structural parameter (or parameters) characterizing the degree of the symmetry distinction between coexisting phases should also be introduced. The structural parameter is different for different systems. It is a long-range order (l.r.o.) parameter if the intermetallic precipitate phase is an ordered phase (for example, in Ni-based superalloys such as Ni–Al and Ni–Ti, or in Al–Li system). It is a displacive mode if a product phase is formed by a crystal lattice rearrangement like the f.c.c. → b.c.c. Bain distortion (for example, precipitation of the B2 γ phase in the f.c.c. α phase in Cu–Be alloys). When the free energy depends on both the composition and the structural parameter, the nonequilibrium free energy can be imaged as a 3-D surface, defined on the composition-structural parameter coordinate plane. The transformation path is determined by two factors, the thermodynamic driving force "pushing" the transformation towards structural states with lower free energy and the kinetics determining the relative speed of compositional and structure parameter relaxations. The kinetics "selects" one between many possible paths that reduce the free energy.

In this paper we consider a situation when one of the product phases formed due to decomposition of a disordered solid solution is an ordered intermetallic phase. In this case the structural parameter is a l.r.o. parameter. For the ordering transition of the first kind, a typical geometry of the free energy surface of a system is shown in Fig. 1(a). For the important case of the f.c.c. Al–Li alloys, in particular, the low temperature thermodynamic stability analysis by Khachaturyan et al. [1] predicted a cascade of structural transformations during decomposition of a disordered alloy into a mixture of a disordered matrix and an ordered intermetallic. The transformation starts from the congruent ordering occurring either by nucleation and growth of the ordered phase domains with the same composition as the disordered phase matrix or by homogeneous barrierless ordering. The resultant single-phase nonstoichiometric ordered state decomposes into a mixture of two ordered phases with the solute-lean ordered phase later spontaneously disordering. The conventional nucleation-and-growth mechanism of the precipitation of the
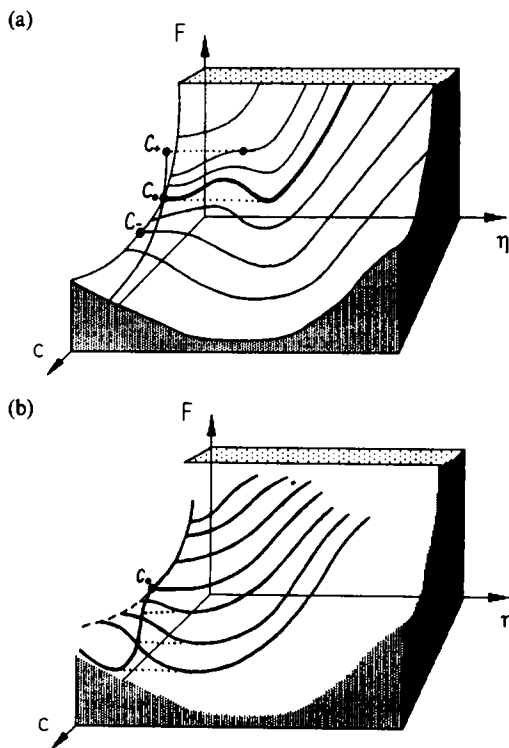

Fig. 1. Schematic dependence of free energy on composition and l.r.o. parameter. (a) The case of the ordering transition of the first kind; (b) The case of the ordering transition of the second kind.

$\delta'(L1_2)$ phase from the disordered f.c.c. solution is also possible but it may occur only within a certain narrow part of the two-phase field. These predictions are confirmed by Sato, Tanaka and Takahashi [2], and Rudmilovich et al. [3] who observed a transient nonstoichiometric ordered single-phase on the high resolution electron microscopic images after quenching Al–Li alloys into the low temperature part of the two-phase region. Shaiu et al. also concluded that the congruent ordering occurs prior to the decomposition by measuring the composition across the ordered domains [4].

The original paper [1] was based on the mean-field approximation. The mean-field approximation works well at low temperatures which is an area of interest for essentially all practically technological applications. The approximation becomes more accurate if interatomic interaction is long-range. However, all qualitative conclusions obtained in [1] are valid regardless of the approximation as long as the mean-field free energy provides qualitatively correct geometry of the free energy surface shown in Fig. 1(a). The same conclusions also follow from a very elegant geometrical approach by Laughlin and Soffa [5]. This approach emphasizes the general rather than specific geometrical characteristics of the free energy surface shown in Fig. 1(a) and, thus, is applied to arbitrary systems. Therefore, the cascade of reactions along the decomposition path predicted for a particular case of $L1_2$ formed by ordering

transition of the first kind in [1] and for more general cases in [5] should be expected for any decomposing system where the ordering is of the first kind. It is expected even for a system where an ordered phase is metastable and does not appear on the equilibrium diagram at all.

In the case where the ordering is an ordering transition of the second kind, a similar but simpler transformation path describing formation of a non-stoichiometric ordered phase prior to the secondary decomposition in a two-phase field of the diagram, is expected [6, 7]. A typical free energy vs composition and l.r.o. parameter hypersurface is shown in Fig. 1(b). The thermodynamics of phase transformations involving both ordering transition of the second kind and conditional spinodal decomposition of the ordered phase have been discussed by Semenovskaya [8], Allen and Cahn [6], Kubo and Wayman [9] and Soffa and Laughlin [7].

Although the thermodynamic stability analysis supplemented by some simple qualitative assumptions concerning the transformation kinetics gives the general features of the decomposition path, its detail description can be obtained only in the framework of a kinetic theory. The kinetic theory should be able to describe different concurrent processes such as ordering, antiphase domain boundary movement, concentration delamination and coarsening in terms of a temporal evolution of composition and l.r.o. parameter profiles. Such a theory formulated in terms of the crystal lattice site diffusion in a nonideal solid solution, which is actually a random walk problem for a system of interacting atoms, has been proposed by Khachaturyan [10, 11]. The kinetic equations obtained in [10] are microscopic counterparts of the continuum Cahn–Hilliard equations [12]. They describe simultaneously the diffusion kinetics of decomposition and ordering in a spatially inhomogeneous system where composition and l.r.o. parameter are coupled by a nonequilibrium free energy. The problem is that the microscopic kinetic equations formulated in [10] are actually nonlinear finite difference differential equations which can be solved only numerically using a computer simulation technique. The purpose of this paper is an investigation of temporal structural transformations of a parent disordered phase quenched into a two-phase field of the equilibrium diagram by solving the nonlinear microscopic diffusion equations. It is an attempt to simulate such different diffusion processes as ordering, decomposition and coarsening simultaneously within the framework of the same physical model. We start our investigation considering two two-dimensional (2-D) binary alloy systems since it dramatically reduces the computational time but nevertheless reasonably well describes all principal features of the process. Three-dimensional extension does not introduce any additional mathematical or physical difficulties. It just requires longer computational time. The corresponding work is under way.

2. THE DECOMPOSITION KINETICS MODEL

In our kinetic model, the atomic structure and alloy morphologies are described by a single-site occupation probability function, $n(\mathbf{r}, t)$, which is actually an average of the occupation number, $c(r)$, over the time-dependent ensemble $n(\mathbf{r}, t) = \langle c(\mathbf{r}) \rangle$, where $\langle \ldots \rangle$ denotes averaging

$$c(\mathbf{r}) = \begin{cases} = 1, & \text{if a site } \mathbf{r} \text{ is occupied by a} \\ & \text{solute atom} \\ = 0, & \text{otherwise.} \end{cases}$$

Following [10], we present the microscopic kinetics equations as Onsager equations in which relaxation parameters are occupation probabilities, $n(\mathbf{r}, t)$, for a solute atoms to be in a crystal lattice site, $\mathbf{r}$, at the time, t. Then the evolution rate, $dn(\mathbf{r}, t)/dt$, is proportional to the thermodynamic driving force, $\delta F/\delta n(\mathbf{r}, t)$, where F is the free energy

$$\frac{dn(\mathbf{r}, t)}{dt} = \sum_{\mathbf{r}'} L(\mathbf{r} - \mathbf{r}') \frac{\delta F}{\delta n(\mathbf{r}', t)} \qquad (1)$$

where $L(\mathbf{r} - \mathbf{r}')$ are kinetic coefficients proportional to the probability of an elementary diffusional jump from site $\mathbf{r}$ to $\mathbf{r}'$ during the time unit. Kinetic coefficients, $L(\mathbf{r} - \mathbf{r}')$ are assumed to be independent of occupation probabilities, $n(\mathbf{r})$. It is actually equivalent to an assumption that atom mobilities or diffusion coefficients are independent of composition. This is a conventional approximation for diffusional kinetics. It may affect the transformation rate but not a sequence of the structural transformations which is our primary concern here.

The Fourier transform of equation (1) gives its reciprocal space representation

$$\frac{d\tilde{n}(\mathbf{k}, t)}{dt} = \tilde{L}(\mathbf{k}) \left\{ \frac{\delta F}{\delta n(\mathbf{r}, t)} \right\}_{\mathbf{k}} \qquad (2)$$

where $\tilde{n}(\mathbf{k}, t)$, $\tilde{L}(\mathbf{k})$, $\{\delta F/\delta n(\mathbf{r})\}_{\mathbf{k}}$ are the Fourier transforms of the relevant functions, $n(\mathbf{r}, t)$, $L(\mathbf{r})$ and $\delta F/\delta n(\mathbf{r})$, defined as

$$\tilde{f}(\mathbf{k}) = \sum_{\mathbf{r}} f(\mathbf{r}) \exp(-i\mathbf{k}\mathbf{r}).$$

From equation (2), we can see that equation (1) describes evolution of both macroscopic and atomic scale concentration inhomogeneities. For a macroscopic scale inhomogeneities, a longwave limit transition transforms equation (1) into the conventional Cahn–Hilliard continuum equation of the macroscopic diffusion with $\delta F/\delta n(\mathbf{r}, t) \to \mu(\mathbf{r})$, where $\mu(\mathbf{r})$ is a local value of the chemical potential. The diffusion coefficient appears as the first nonvanishing term of the long wave expansion of $\tilde{L}(\mathbf{k})$ ($\tilde{L}(\mathbf{k}) \to -Bk^2$ where B is the diffusional mobility of a solute atom related to its diffusivity, D, by the Einstein equation, $B = Dc(1 - c)/k_B T$, k_B is the Boltzmann constant, T is the temperature and c is an average solute atom composition; the zero expansion term, $\tilde{L}_0(0)$, vanishes because of the conservation of the number of atoms [11]). Equation (1), being microscopic, also describes

the long-range order which is actually an atomic scale modulation of the average alloy composition, c, with the superstructure periods.

For the computer simulation we must specify the parameters of the phenomenological kinetic equations (1) and (2), and the nonequilibrium free energy functional, in particular. We are primarily interested in qualitative rather than quantitative physical results. Because of that, it is sufficient to choose the free energy in a simplest possible form if this form provides the qualitatively correct geometry of the free energy surface defined on the composition-l.r.o. parameter plane as shown in Fig. 1. Such a geometry gives the qualitatively correct temperature dependence of the l.r.o. parameters above and below the ordering transition temperature, a two-phase field at low temperatures and properly describes the instability lines and lines of the metastable equilibrium within the two-phase field of the phase diagram. These instability ranges are the most important features for characterization of the sequence of structural states formed during a decomposition of a quenched disordered alloy. The mean-field free energy functional

$$F = \tfrac{1}{2} \sum_{r'r''} W(r' - r'') n(r')n(r'')$$
$$+ k_B T \sum_{r'} [n(r')\ln n(r')$$
$$+ (1 - n(r'))\ln(1 - n(r'))] \qquad (3)$$

[$W(r' - r'')$ is the interaction energy between a pair of atoms at r' and r''], meets the above-formulated requirements in spite of its simplicity. It correctly determines the sequence of structural states along the transformation path although the rates of the transformations of these states are not necessarily very accurate.

The free energy (3) is actually a good approximation for the case of a long-range interaction and at low temperatures [13]. Using the free energy (3), the kinetic equation (2) reads

$$\frac{d\tilde{n}(k, t)}{dt} = L(k)\left[V(k)\tilde{n}(k, t) \right.$$
$$\left. + kT_B\left\{\ln\!\left(\frac{n(r, t)}{1 - n(r, t)}\right)\right\}_k \right] \qquad (4)$$

where $\{\ln(n(r, t)/1 - n(r, t)\}_k$ is the Fourier transform of $\ln(n(r, t)/1 - n(r, t))$, and

$$V(k) = \sum_{r} W(r)\exp(-ikr) \qquad (5)$$

is the Fourier transform of the interaction energies $W(r)$. Equation (4) is a nonlinear equation with respect to the concentration wave amplitudes, $\tilde{n}(k, t)$, where the interaction between amplitudes is described by the nonlinear term in the square brackets. It is valid for an arbitrary long-range interaction model where all information concerning interaction energies enters the Fourier transform (5). It should be empha-

sized that the conventional Cahn–Hilliard equation with a constant coefficient at the gradient term can be obtained only in the mean-field approximation using a long-wave limit. Any correlation effects would immediately result in a dependence of the gradient term coefficient on composition and l.r.o. parameter.

At small k (long-wave limit) $\tilde{n}(k, t)$ describes concentration inhomogeneities while at k close to the superlattice vector, k_0, $\tilde{n}(k, t)$ describes l.r.o. parameter heterogeneities [14]. In the case of precipitation of an ordered phase, the function $\tilde{n}(k, t)$ assumes large values only around $k = 0$, with $|k|$ of the order of $2\pi/d$, where d is a typical size of a concentration segregation, and around $k = k_0$. The fact that $\tilde{n}(k, t)$ assumes considerable values only around $k = 0$ and $k = k_0$ allows one, in principle, also to use an alternative continuum aproximation of equation (1) considering only temporal evolution of smooth composition profiles, $c(r)$ and l.r.o. profiles, $\eta(r)$. They well approximate the function $\tilde{n}(k)$ near $k = 0$ and $k = k_0$, where $\tilde{n}(k)$ is substantial. Then the free energy, F, can be presented in the form of a Landau expansion.

In the simplest case, when the homogeneous ordered phase is described by the only concentration wave with $k = k_0$, where k_0 is a superlattice vector which is a half of a fundamental reciprocal lattice vector of the parent disordered phase, the ordering results in a development of the only concentration wave amplitude, $\tilde{n}(k_0) = Nc\eta$, where η is a l.r.o. parameter. The resultant ordered phase is then described by occupation probabilities [11]

$$n(r) = c + c\eta \exp(ik_0 r). \qquad (6)$$

Equation (6) describes many typical ordered structures such as B2, L1$_0$, L1$_1$.

In this computer simulation study, the set of N nonlinear microscopic kinetics equations (4) are solved for a 2-D lattice model for a supercell with n-crystal lattice sites. Periodic boundary conditions are applied in each of the directions. The initial disordered distribution of solute atoms is described by an occupation probability profile, $n(r, 0)$, which is generated by random number generators. The N differential equations [equation (4)] are solved using the Euler technique

$$\tilde{n}(k, t + \Delta t) = \tilde{n}(k, t) \times \frac{d\tilde{n}(k, t)}{dt} \Delta t \qquad (7)$$

where $d\tilde{n}(k, t)/dt$ is expressed in terms of $\tilde{n}(k, t)$ through the right-hand side of equation (3). The value of the time increment, Δt, in equation (7) is chosen in such a way to ensure the stability and accuracy of the numerical integration. Solution of N microscopic diffusion equations with respect to $\tilde{n}(k, t)$ allows us to find its back-Fourier transform, which is the occupation probability profile, $n(r, t)$, and record its temporal evolution. The function, $n(r, t)$, contains all the information concerning the microstructural transformation along the decomposition path including

congruent ordering, formation of antiphase domains, homogeneous and heterogeneous decomposition and coarsening of ordered phase particles.

3. MODEL SYSTEMS FOR DECOMPOSITION

Below we consider a 2-D binary alloy which is a disordered phase at high temperatures and assumes a two-phase equilibrium between a solute-lean disordered phase and a solute-rich ordered phase at low temperatures. We consider two cases, the first of which is that ordered phase is formed by an ordering transition of the second kind, and the second of which is that the ordered phase is formed by an ordering transition of the first kind.

3.1. Decomposition accompanied by an ordering transition of the second kind

A 2-D binary alloy in a square lattice and a particular set of the interchange energies describing the interactions between atoms

$$w_1 = 1.0 \quad w_2 = -0.8 \quad w_3 = -0.55 \qquad (8)$$

are chosen, where w_1, w_2, and w_3 are the first, second, and third neighbor interchange energies. Interactions beyond the third coordination shell are neglected. The characteristics of the system, ordering or phase separation, or both, upon quenching a homogeneous disordered solid solution, can be determined by an investigation of $V(\mathbf{k})$, which is the Fourier transform of the interchange energy (5) [11, 14]. For a 2-D square lattice, it is

$$V(\mathbf{k}) = 2w_1(\cos 2\pi h + \cos 2\pi l)$$
$$+ 4w_2 \cos 2\pi h \cos 2\pi l$$
$$- 2w_3(\cos 4\pi h + \cos 4\pi l) \qquad (9)$$

where $\mathbf{k} = 2\pi/a\,(h, l)$, $-\frac{1}{2} \leqslant h \leqslant \frac{1}{2}$ and $-\frac{1}{2} \leqslant l \leqslant \frac{1}{2}$ are coordinates of the reciprocal lattice sites within the first Brillouin zone and a is the crystal lattice parameter. For the set of energies (8) the absolute minimum of the function $V(\mathbf{k})$ falls at $\mathbf{k} = \mathbf{k}_0 = 2\pi/a$ ($\frac{1}{2}\frac{1}{2}$). According to the concentration wave method [14], this means that the disordered solution should order at low temperatures, and the atomic structure of the ordered phase is described by occupation probabilities given in equation (6) with

$$\mathbf{k}_0 = \frac{2\pi}{a}\left(\frac{1}{2} \quad \frac{1}{2}\right).$$

Substituting

$$\mathbf{k}_0 = \frac{2\pi}{a}\left(\frac{1}{2} \quad \frac{1}{2}\right)$$

and $\mathbf{r} = a\,(m, n)$, where (m, n) are dimensionless integer coordinates of crystal lattice sites, into (6) gives the occupation probabilities as a function of site coordinates, (m, n)
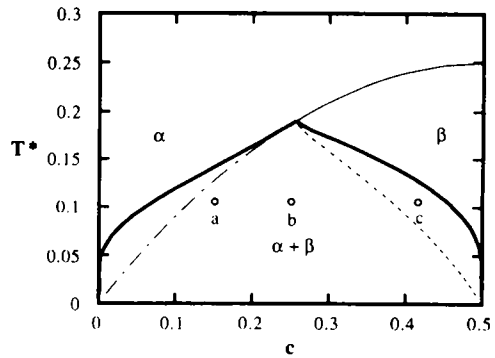
$$n(\mathbf{r}) = c + c\eta \cos \pi(m + n) \qquad (10)$$

Fig. 2. Reduced equilibrium phase diagram for the ordering transition of the second kind. α designates the disordered phase field, β designates the ordered phase field, solid lines are the phase boundaries of the low temperature two-phase field, dot-dashed line is the ordering transition line of the second kind extended into the $\alpha + \beta$ field, thin line is the stable ordering transition line of the second kind, dotted line is the conditional spinodal and letters a, b and c represent the alloy compositions and temperatures chosen for the computer simulation.

which describes the atomic distribution of solute atoms in the ordered phase. Substituting (10) to (3) yields

$$F(c, \eta, T) = N\frac{c^2}{2}V(0) + \frac{N}{2}V(\mathbf{k}_0)(c\eta)^2$$
$$+ N\frac{k_B T}{2}[(c + c\eta)\ln(c + c\eta)$$
$$+ (1 - c - c\eta)\ln(1 - c - c\eta)$$
$$+ (c - c\eta)\ln(c - c\eta)$$
$$+ (1 - c + c\eta)\ln(1 - c + c\eta)] \qquad (11)$$

where N is the total number of lattice sites. Minimizing the function $F(c, \eta, T)$ with respect to η at a given composition, c, gives the equilibrium l.r.o. parameter $\eta(c, T)_0$ at the congruent ordering. Its substitution to (11) yields the equilibrium free energy, $F[c, \eta(c)_0]$,
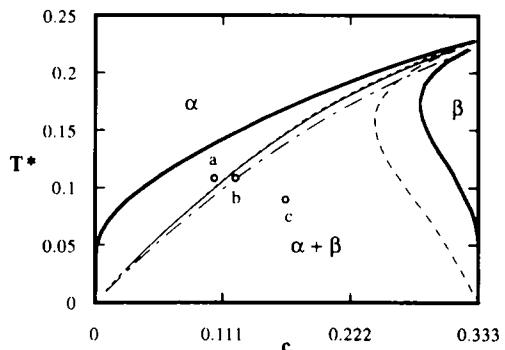

Fig. 3. Reduced equilibrium phase diagram for ordering transition of the first kind. α is the disordered phase, β is the ordered phase, thick solid lines are phase boundaries, dot-dahsed line is the ordering instability curve (T_-), dashed line is the conditional spinodal, dotted line is the disordering instability curve (T_+), and the thin solid line is the T_0 line where the free energies of the ordered and disordered phases are equal.

which becomes a function of composition only. The conventional common-tangent construction for the F vs c curves at different temperatures determines the equilibrium compositions of the disordered α phase and the ordered β phase and allows one to draw the solubility lines. The calculated phase diagram is presented in Fig. 2. The diagram shows an ordering transition line of second kind terminated by the tricritical point at $c = 0.255$ and $T^* = 0.19$ below which there is a two-phase field describing equilibrium between a disordered and an ordered phase. Reduced temperature $T^* = k_B T/|V(\mathbf{k}_0)|$ is used in the phase diagram representation. This phase diagram is topologically very similar to the upper part of the Fe–Al diagram describing the two-phase field, the disordered + ordered B2 phase [15].

3.2. Decomposition accompanied by an ordering transition of the first kind

A binary alloy in a 2-D close-packed triangle lattice and a particular set of interchange energies

$$w_1 = 1.0, \quad w_2 = -1.0, \quad w_3 = 0.5, \quad w_4 = 0.25,$$

$$w_5 = -0.5, \quad w_6 = -0.25 \quad (12)$$

are chosen where w_i is the ith neighbor interchange energies ($i = 1, 2, \ldots 6$), respectively. Interactions beyond the six coordination shell are assumed to be zero. $V(\mathbf{k})$, the Fourier transform of the interchange energy, in a 2-D triangular lattice is then presented as

$$V(\mathbf{k}) = 2w_1[\cos 2\pi h + \cos(2\pi l) + \cos(h - l)]$$

$$+ 2w_2[\cos 2\pi(h + 1) + \cos 2\pi(h - 2l)$$

$$+ \cos 2\pi(2h - l)] + 2w_3[\cos 4\pi h$$

$$+ \cos 4\pi l + \cos 4\pi(h - l)]$$

$$+ 2w_4[\cos 2\pi(2h + l) + \cos 2\pi(h + 2l)$$

$$+ \cos 2\pi(h - 3l)] + 2w_5[\cos 6\pi h$$

$$+ \cos 6\pi l + \cos 6\pi(h - l)]$$

$$+ 2w_6[\cos 4\pi(h + l) + \cos 4\pi(h - 2l)$$

$$+ \cos 2\pi(2h - l)]$$

$\mathbf{k} = 2\pi(h\mathbf{a}_1^*, l\mathbf{a}_2^*)$, h and l are dimensionless coordinates of the reciprocal lattice sites within the range, $-\frac{1}{2} \leqslant h \leqslant \frac{1}{2}$ and $-\frac{1}{2} \leqslant l \leqslant \frac{1}{2}$, $\mathbf{a}_1^*$ and $\mathbf{a}_2^*$ are unit vectors in the reciprocal space forming an angle $120°$ to each other. With interaction parameters (12) the absolute minimum of the function $V(\mathbf{k})$ falls at $\mathbf{k} = \pm\mathbf{k}_0 = \pm2\pi/3\,(\mathbf{a}_1^* - \mathbf{a}_2^*)$. Therefore, occupation probabilities describing the ordered phase are

$$n(\mathbf{r}) = c + c\eta\,[\exp(i\mathbf{k}_0\mathbf{r}) + \exp(-i\mathbf{k}_0\mathbf{r})] \quad (13)$$

where $\mathbf{r} = (m\mathbf{a}_1, n\mathbf{a}_2)$, m, n are dimensionless integer coordinates of crystal lattice sites and $\mathbf{a}_1$, $\mathbf{a}_2$ are unit cell vectors in the real space. Substituting $\mathbf{k}_0$ and $\mathbf{r}$ into (13) gives the occupation probabilities of finding

solute atoms at site $\mathbf{r}$ as a function of the integer site coordinates, (m, n)

$$n(\mathbf{r}) = c + 2c\eta \cos\frac{2\pi}{3}(m - n). \quad (14)$$

Equation (14) describes the atomic structure of the ordered phase. The corresponding mean-field free energy is given by

$$F(c, \eta, T) = N\frac{c^2}{2}V(0) + NV(\mathbf{k}_0)(c\eta)^2$$

$$+ \frac{Nk_B T}{3}[(c + c\eta)\ln(c + 2c\eta)$$

$$+ (1 - c - 2c\eta)\ln(1 - c - 2c\eta)$$

$$+ 2(c - c\eta)\ln(c - c\eta)$$

$$+ (1 - c + c\eta)\ln(1 - c - c\eta)]. \quad (15)$$

The calculated phase diagram based on the free energy (15) is shown in Fig. 3. Reduced temperature in Fig. 3 is defined as $T^* = k_B T/|V(\mathbf{k}_0)|$. The free energy provides an ordering transition of the first kind. The completely ordered compound has a stoichiometric formula of A_2B.

4. COMPUTER SIMULATION RESULTS

4.1. Decomposition with an ordering transition of the second kind

In this computer simulation, a 2-D square lattice consisting of 64×64 unit cells is used. The starting occupation probabilities correspond to a completely disordered state with small random perturbations. Several compositions representing different parts of the two-phase field in the phase diagram in Fig. 2
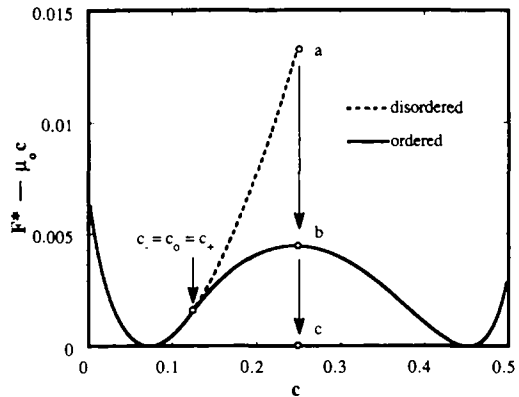

Fig. 4. Reduced free energy as a function of composition for both the ordered and disordered phases at $T^* = 0.106$ in the case of ordering transition of the second kind. The dotted line is a segment of the free energy curve of the disordered phase in the absolutely unstable region. $\mu_0 = \partial F/\partial c_\alpha = \partial F/\partial c_\beta$ is the equilibrium chemical potential, $c_- = c_+ = c_0$ is the composition at which the ordering transition of the second kind occurs at $T^* = 0.106$. Point a is the free energy of the disordered phase at composition 0.25, point b is the free energy of the congruently ordered phase and point c is the free energy of the final two-phase equilibrium state.

were chosen for studying the decomposition kinetics. They are "quenched" into the two-phase field at temperature $T^* = 0.106$. The free energy curves for both the disordered and ordered states at $T^* = 0.106$ are shown in Fig. 4.

For the substitutional diffusion in alloys, the elementary diffusion jump probabilities, $L(\mathbf{r})$, are assumed to be nonzero at $\mathbf{r} = 0$ and at $\mathbf{r}$ corresponding to the nearest neighbor sites only.

Using this assumption and the requirement,

$$\tilde{L}(0) = \sum_{\mathbf{r}} L(\mathbf{r}) = 0,$$

which follows from the conservation of the number of atoms, we obtain

$$\tilde{L}(\mathbf{k})_0 = -4L_1(\sin^2\pi h + \sin^2\pi l) \qquad (16)$$

where L_1 is the jumping probability between nearest neighbor sites during a unit of time. It is convenient to introduce the dimensionless reduced time, t^*, measured in terms of the typical time of an elementary diffusion event, $t_0^* = 1/L_1$, by relation

$$t^* = t/t_0^*. \qquad (17)$$

The diffusion kinetics described by equation (4) occurs very fast in the beginning of the decomposition process and much slower at the later stages. Because of that, the time increment, Δt^*, in equation (7) has been chosen differently at different stages.

4.1.1. Composition $c = 0.25$. This composition, labeled by point b in Fig. 2, is almost the middle point between the equilibrium compositions of the disordered and ordered phases at temperature $T^* = 0.106$. The temporal evolution of the occupation probabilities $n(\mathbf{r}, t)$ at four different times during the aging process is illustrated by Fig. 5(a–d). In Fig. 5 and the figures followed, the values of occupation probabilities of finding solute atoms B, which describe the atomic structure, are imaged by different darkness of the circles at crystal lattice sites.

Our initial state ($t^* = 0$) is a quenched completely disordered solution. Its free energy is represented by point a in Fig. 4. At time close to $t^* = 2.0$, the whole system proves to be at an ordered single-phase state consisting of a set of antiphase domains [Fig. 5(a)]. An alternation of dark and light circles in Fig. 5 and all other figures indicates the atomic pattern of the ordered phase. The free energy of the congruently ordered state is shown by point b in Fig. 4. The structure of the ordered phase coincides with that described in Section 3 for the concentration wave analysis with the superlattice vector

$$\mathbf{k}_0 = \frac{2\pi}{a}\left(\frac{1}{2}, \frac{1}{2}\right).$$

Because the ordering reaction does not affect the composition of the alloy, the ordering is a congruent reaction and, thus, the ordered phase is nonstoichiometric. The occupation probabilities away from the antiphase domain boundaries have values very close

to the congruent equilibrium values, $n_1 \approx c + c\eta_0$ and $n_2 \approx c - c\eta_0$ following from equation (10). As is expected, the congruent ordering leads to the growth of the amplitude, $\tilde{n}(\mathbf{k}_0) = Nc\eta$, and disappearance of all other amplitudes. It may be noticed that the distribution of antiphase domains shows a remarkable resemblance to experimental observations in ordering systems (see, for example, [6]).

The nonstoichiometric ordered phase formed by the congruent ordering reaction was found to be unstable with respect to the phase decomposition into an ordered and disordered phase mixture. An important computer simulation result which should be especially emphasized is that the decomposition process following the congruent ordering occurs predominantly at the APBs. The reduction of the composition at the APBs towards the equilibrium value $c = c_\alpha = 0.074$ and subsequent gradual APB disordering are observed. The composition of the ordered phase moves towards the equilibrium value $c_\beta = 0.454$ at the same time. It is illustrated by Fig. 5(b) for $t^* = 25$, in which the APBs are replaced by layers of the disordered α phase. Very small ordered domains disappear quickly and become spherical disordered particles as a result of simultaneous decomposition at APBs and coarsening.

Figure 5(c), corresponding to $t^* = 200$, demonstrates the growth of the disordered layer thickness between the antiphase domains. At this stage, the decomposition has almost reached its completion. The microstructure is a mixture of ordered and disordered phases with the equilibrium values of the composition and l.r.o. parameter. At $t^* = 200$, the coarsening reducing the area of order/disorder interface, however, is still far from completion. The reduction of interfacial area is accomplished through both surface diffusion along the order–disorder interface and the bulk diffusion across the disordered layer and across the ordered domains.

The result of coarsening is shown in Fig. 5(d). This microstructure has much less interfacial area compared to that shown in Fig. 5(c). The resulting amount of the ordered and disordered phases are found to be in agreement with the lever rule, which is about 50% each at this relevant composition and temperature. The total free energy of the two-phase equilibrium system is represented by point c in Fig. 4.

4.1.2. Composition $c = 0.15$. This composition is close to the solubility curve of the disordered phase (see point a in Fig. 2). The occupation probabilities represented by gray levels are plotted in Fig. 6(a–d) for four different reduced times. The transformation starts as a congruent ordering, which produces a transient nonstoichiometric ordered single-phase with antiphase domain boundaries at $t^* = 10$ [Fig. 6(a)]. The occupation probabilities within the ordered domains are close to congruent equilibrium values at $c = 0.15$. The ordered phase shown in Fig. 6(a) has experienced substantial coarsening of antiphase domains occurring simultaneously with ordering prior to any
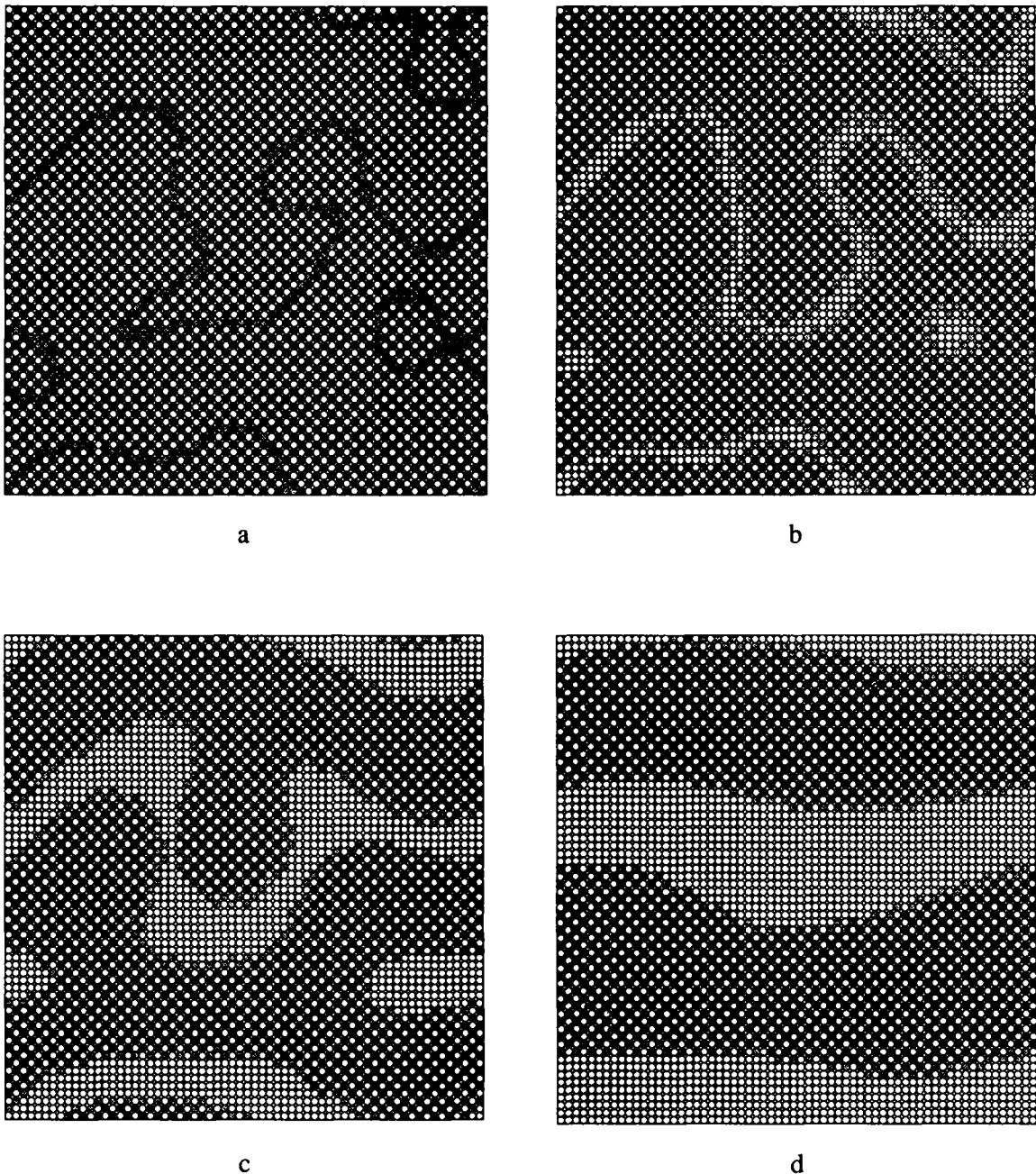
a

b

c

d

Fig. 5. Temporal evolution of occupation probabilities at temperature $T^* = 0.106$ and composition 0.25 in the case of the ordering transition of the second kind. The magnitudes of the occupation probabilities at lattice sites are visualized by the darkness of the circles at the crystal sites. Occupation probabilities close to 1.0 are represented by the darkest circles and those close to 0.0 are represented by the lightest circles. (a) $t^* = 2$; (b) $t^* = 25$; (c) $t^* = 200$; (d) $t^* = 1000$.

significant concentration redistribution. It is driven by the reduction of the total APB energy. The size of domains is much larger in Fig. 6(a) than in Fig. 5(a).

The single-phase state shown in Fig. 6(a) is also unstable with respect to further decomposition. At $t^* = 50$, the disordered phase starts to appear at the APBs, whereas the composition of ordered regions close to the APBs moves towards the equilibrium values of the ordered phase. Following the appearance of disordered phase at APBs, disordered phase

also develops inside the domains. Ordered domains near the high curvature regions of the APBs first reach the equilibrium composition of the ordered phase. At $t^* = 300$, the decomposition already reaches its completion. The resultant two-phase morphology consists of spherical equilibrium ordered phase particles in the disordered matrix [Fig. 6(c)].

Further coarsening of the two-phase mixture of Fig. 6(c) is, unlike the coarsening of the antiphase domains, a very slow process. It is driven by the
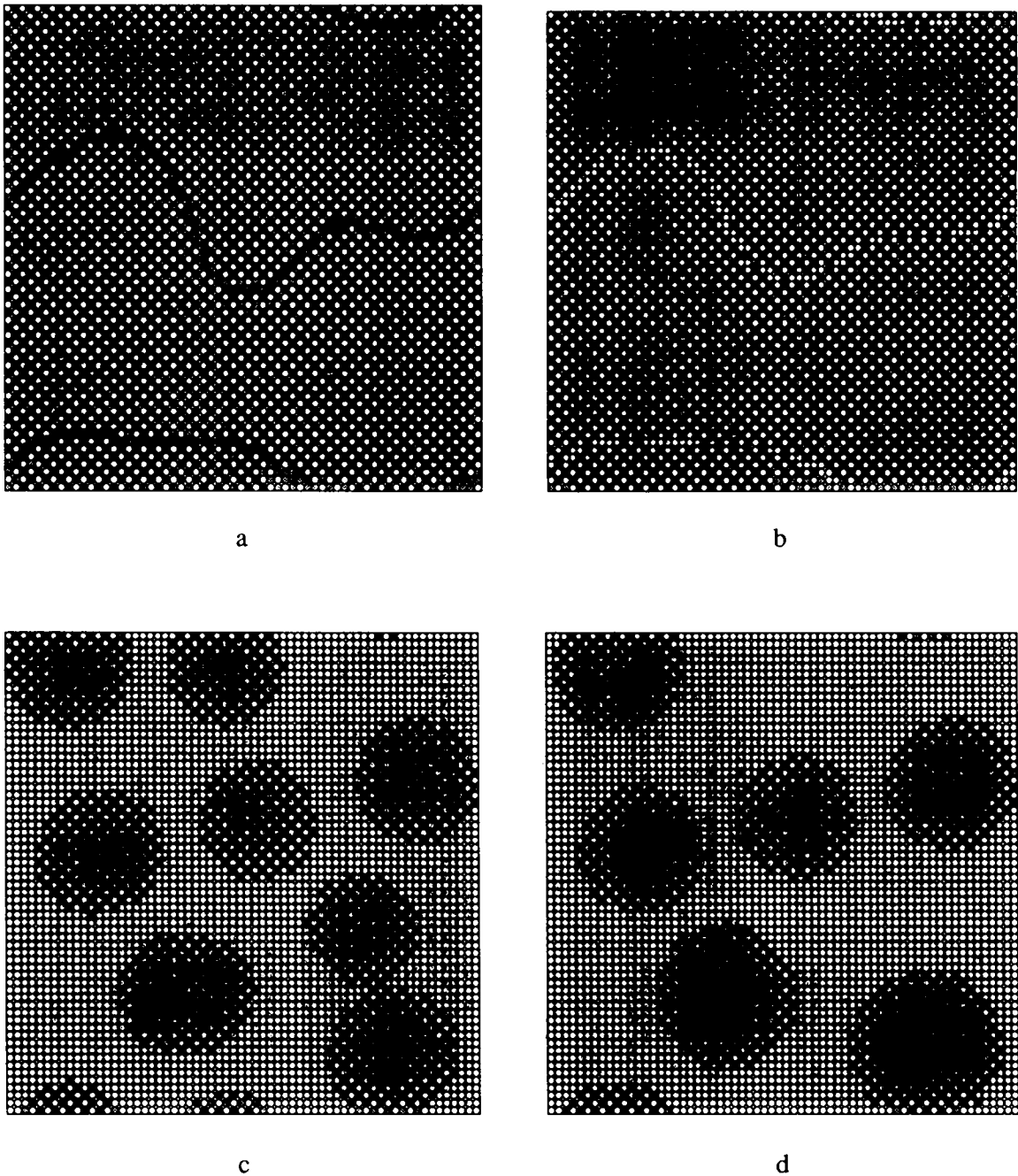
a

b

c

d

Fig. 6. Temporal evolution of occupation probabilities at temperature $T^* = 0.106$ and composition 0.15 in the case of ordering transition of the second kind. Representation of the occupation probabilities is the same as Fig. 5. (a) $t^* = 10$; (b) $t^* = 50$; (c) $t^* = 300$; (d) $t^* = 1000$.

reduction of the order/disorder interfacial energy and is determined by the long-range diffusion. The microstructure produced by the coarsening is shown in Fig. 6(d) for $t^* = 1000$. In Fig. 6(d), the number of ordered phase particles is reduced as they become larger, compared to Fig. 6(c).

4.1.3. Composition c = 0.415. This composition is between the conditional spinodal line and equilibrium solubility line of the ordered phase in the phase diagram (point c in Fig. 2). This means that completely ordered state with nonstoichiometric

composition can not spinodally decompose. The decomposition of a quenched disordered phase, again, starts from the congruent ordering, which is finished at around $t^* = 1.0$ [Fig. 7(a)].

After the congruent ordering, a disordered layer arises at the antiphase domain boundaries [Fig. 7(b)]. Heterogeneities within the ordered domains do not lead to any homogeneous decomposition. They disappear producing uniform ordered domains. At $t^* = 100$, the decomposition process already reaches its completion Fig. 7(c)].
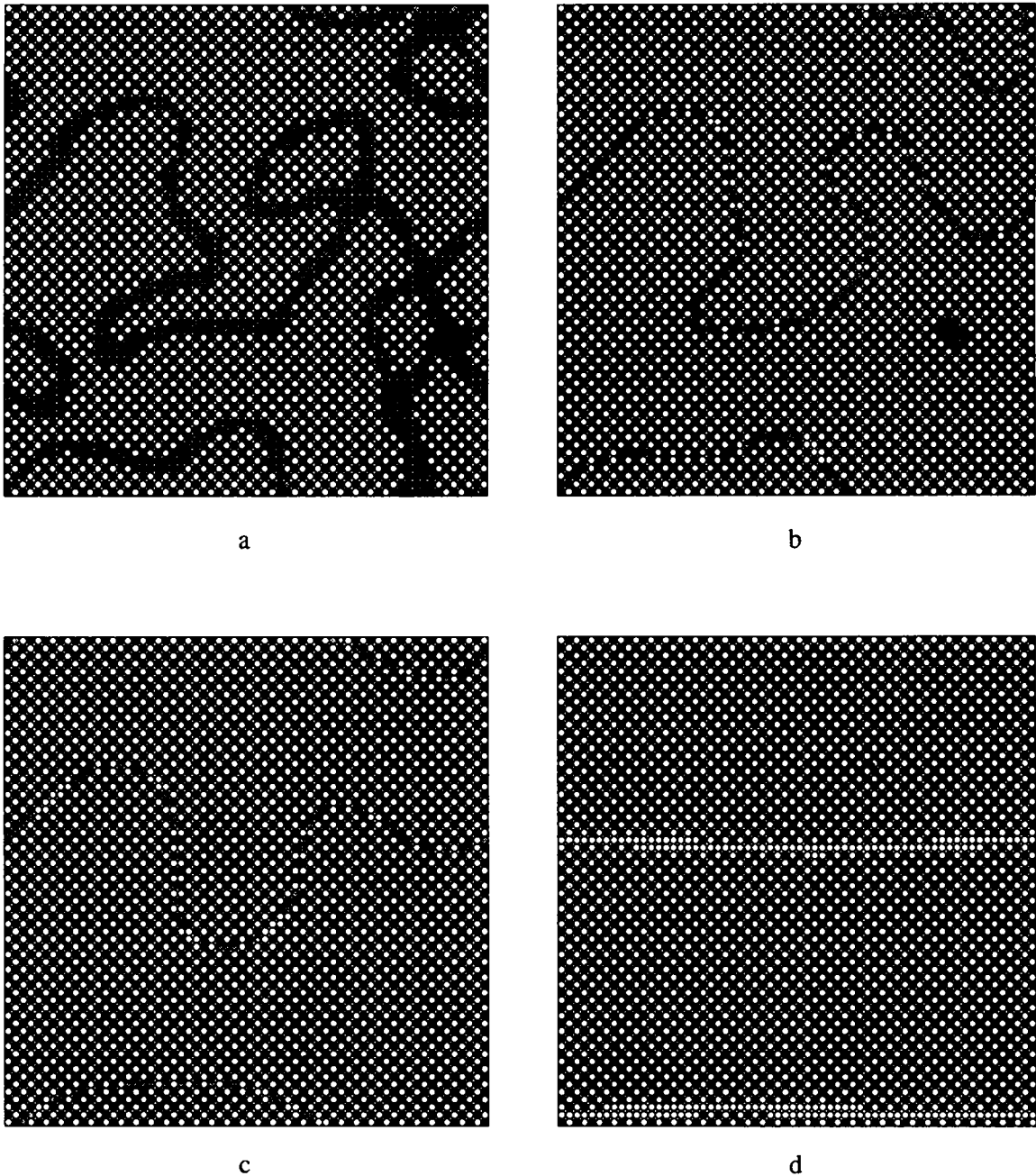
a

b

c

d

Fig. 7. Temporal evolution of occupation probabilities at temperature $T^* = 0.106$ and composition 0.415 in the ordering transition of the second kind. Representation of the occupation probabilities is the same as Fig. 5. (a) $t^* = 1.0$; (b) $t^* = 5$; (c) $t^* = 25$; (d) $t^* = 500$.

The final stage is the coarsening which leads to a microstructure shown in Fig. 7(d) where a thin layer of disordered phase wetting the APBs is observed.

4.2. Decomposition with the ordering transition of the first kind

In this computer simulation, a 2-D close-packed triangular lattice with 48×48 unit cells is employed. Compositions used in this study are indicated by points a, b and c in the phase diagram (Fig. 3). They are $c = 0.103$ and 0.123, which are "quenched" into the two-phase field at the temperature $T^* = 0.109$

(points a and b), and $c = 0.165$ (point c) at lower temperature, $T^* = 0.90$. With $T^* = 0.9$, we can obtain all three possible antiphase domains for $c = 0.165$ using the system size of 48×48 unit cells. The free energy curves for both, the disordered and the ordered state at temperature, $T^* = 0.109$, are shown in Fig. 8.

For the substitutional diffusion the nearest-neighbor jump approximation for $L(r)_0$ can be employed. Then the Fourier transform of $L(r)$ is

$$\tilde{L}(\mathbf{k}) = -4L_1[\sin^2\pi h + \sin^2\pi l + \sin^2\pi(h-l)] \quad (18)$$
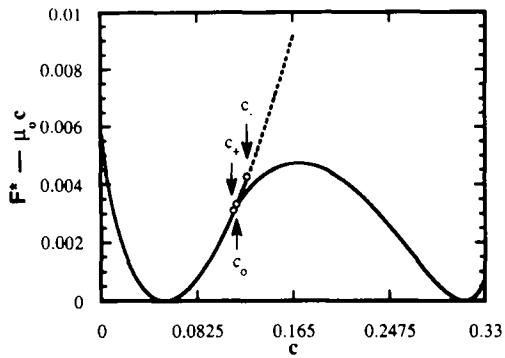
Fig. 8. Reduced free energy as a function of composition for both the ordered and disordered phases at $T^* = 0.109$ in the case of the ordering transition of the first kind, the dotted line is a segment of the free energy curve of the disordered phase in the absolutely unstable region. c_- Is the ordering instability composition, c_+ is the disordering instability composition and c_0 is the composition at which the free energies of the disordered and ordered phases are equal. $\mu_0 = \partial F/\partial c_\alpha = \partial F/\partial c_\beta$ is the equilibrium chemical potential.

where reciprocal lattice point coordinates, (h, l), are related to the vector $\mathbf{k}$ as

$$\mathbf{k} = \frac{2\pi}{a}(h\mathbf{a}_1^* + l\mathbf{a}_2^*)$$

where $\mathbf{a}_1^*$ and $\mathbf{a}_2^*$ arc the unit reciprocal lattice vectors of the real triangular lattice.

4.2.1. Composition $c = 0.165$, $T^* = 0.9$. This composition is roughly in the middle of the two-phase field of ordered and disordered phases at temperature $T^* = 0.9$ (point c in Fig. 3). The "as-quenched" occupation probabilities correspond to the completely disordered state. Figure 9(a–d) shows various stages of overall decomposition processes. In the very initial stage the congruent ordering occurs due to the growth of the amplitudes of the concentration waves with the wave vectors

$$\pm\mathbf{k}_0 = \pm\frac{2\pi}{3}(\mathbf{a}_1^* - \mathbf{a}_2^*).$$

These wave vectors coincide with those minimizing the function $V(\mathbf{k})$. The obtained ordered phase has a structure predicted by equations (13) and (14). The developed amplitudes are actually proportional to the l.r.o. parameter η. At time $t^* = 2.5$ an ordered single-phase state arrived with all three possible antiphase domains [Fig. 9(a)]. Although the l.r.o. parameter is inhomogeneous because of appearance of APBs, the composition is almost uniform throughout the system. The occupation probabilities within the ordered phase domains are close to the equilibrium values for the congruent ordering at composition $c = 0.165$.

This system also demonstrates the compositional instability at APBs. At time $t^* = 10$, the decomposition at APBs produces disordered phase film separating the antiphase domains [Fig. 9(b)]. Figure 9(c), corresponding to $t^* = 100$, illustrates the growth of the disordered layers between antiphase domains, with the l.r.o. parameter and composition of the

ordered phase moving towards the equilibrium values. One ordered domain has been eliminated during the decomposition due to simultaneous coarsening.

At $t^* = 500$, another domain disappears due to coarsening and the final microstructure is formed. It is a mixture of a single domain ordered phase and a disordered matrix with equilibrium composition and l.r.o. parameter [Fig. 9(d)].

4.2.2. Composition $c = 0.123$, $T^* = 0.109$. For this composition and temperature the representative point of the system is located between the T_0 and T_- lines (point b in Fig. 3), i.e. within the field where the quenched disordered phase is metastable (stable with respect to infinitesimal fluctuations of the l.r.o. parameter and composition). Our computer simulation shows that the small random fluctuations introduced into the initial occupation probability distribution decay as a function of time, which is in agreement with thermodynamics of the system. Because of this, we introduced large fluctuations into the system in the form of critical nuclei of the congruent ordered domains with the same composition as the initial disordered phase and with the equilibrium l.r.o. parameter corresponding to the given temperature and composition. The congruent nuclei of 19 atoms with a radius $2a$ disappear while those of 37 atoms with a radius $3a$ grow. Therefore, the critical radius of nucleus is close to $3a$. Four nuclei of radius $3a$ were randomly placed in the initial occupation probability distribution corresponding to the disordered state.

The temporal evolution of the occupation probabilities in this situation is shown in Fig. 10(a–d). The initial occupation probability distribution describing four nuclei of the congruently ordered phase in the disordered matrix is shown in Fig. 10(a). Initially the values of the l.r.o. parameter decrease inside each nucleus due to the relaxation of l.r.o. parameter profiles. This process produces very diffuse interfaces between the nuclei and matrix. The "tails" of l.r.o. parameter profiles for different nuclei interact with each other. The competition between different antiphase nuclei during coarsening results in disappearance of three nuclei and growth of the remaining one. Its growth occurs congruently, producing a single domain crystal at time $t^* = 18$ [Fig. 10(b)]. This congruent growth produces a nonstoichiometric ordered phase with approximately the same average composition as the original disordered phase and the same symmetry as the final ordered phase.

This congruently ordered phase proves to be unstable with respect to further isostructural decomposition into two ordered phases [Fig. 10(c)]. Since we have a single domain of the ordered transient phase without APBs, the decomposition occurs only homogeneously via a spinodal mechanism through growth of fluctuations in composition and l.r.o. parameter. This computer simulation result is consistent with the fact that the free energy of the congruently ordered phase resides at the convex part of the free energy vs composition curve for the ordered phase.

a   b

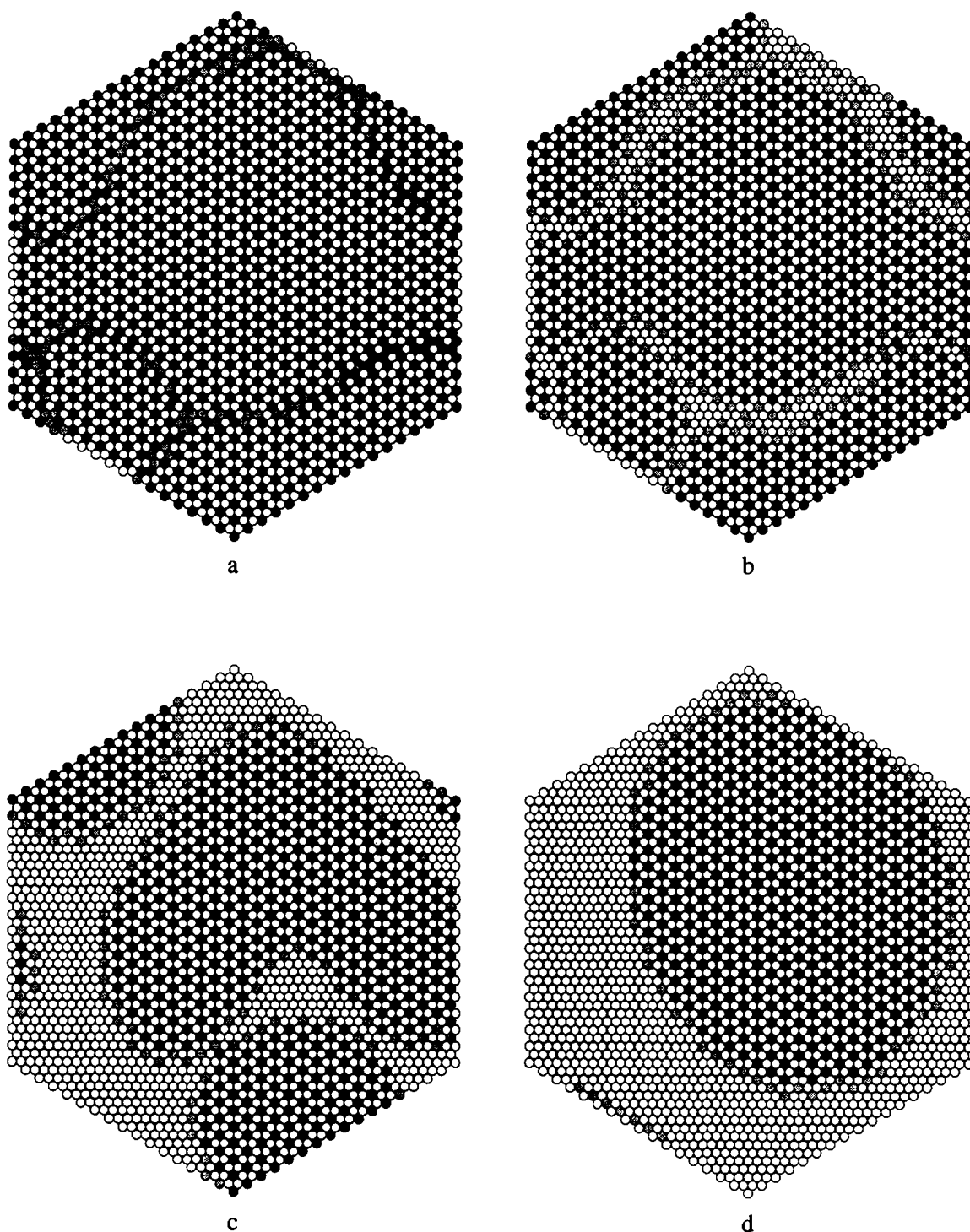c   d

Fig. 9. Temporal evolution of occupation probabilities at lattice sites at composition 0.165 and temperature $T^* = 0.9$ in the ordering transition of the first kind. Representation of the occupation probabilities is the same as Fig. 5. (a) $t^* = 2.5$; (b) $t^* = 10$; (c) $t^* = 100$; (d) $t^* = 500$.

The solute-lean ordered phase resulted from the spinodal decomposition underwent a spontaneous disordering transition around $t^* = 60$ to 70, at which the composition of the solute-lean phase crosses the instability value c_+. It can be noticed in Fig. 10(c), corresponding to $t^* = 100$, that the composition inside the disordered phase is higher than that at the order/disorder interface region, which means that the decomposition is faster at the order/disorder interface than inside the disordered phase where the composition moves towards the equilibrium composition by the conventional growth process.

Further decomposition and coarsening of the microstructure shown in Fig. 10(c) result in a
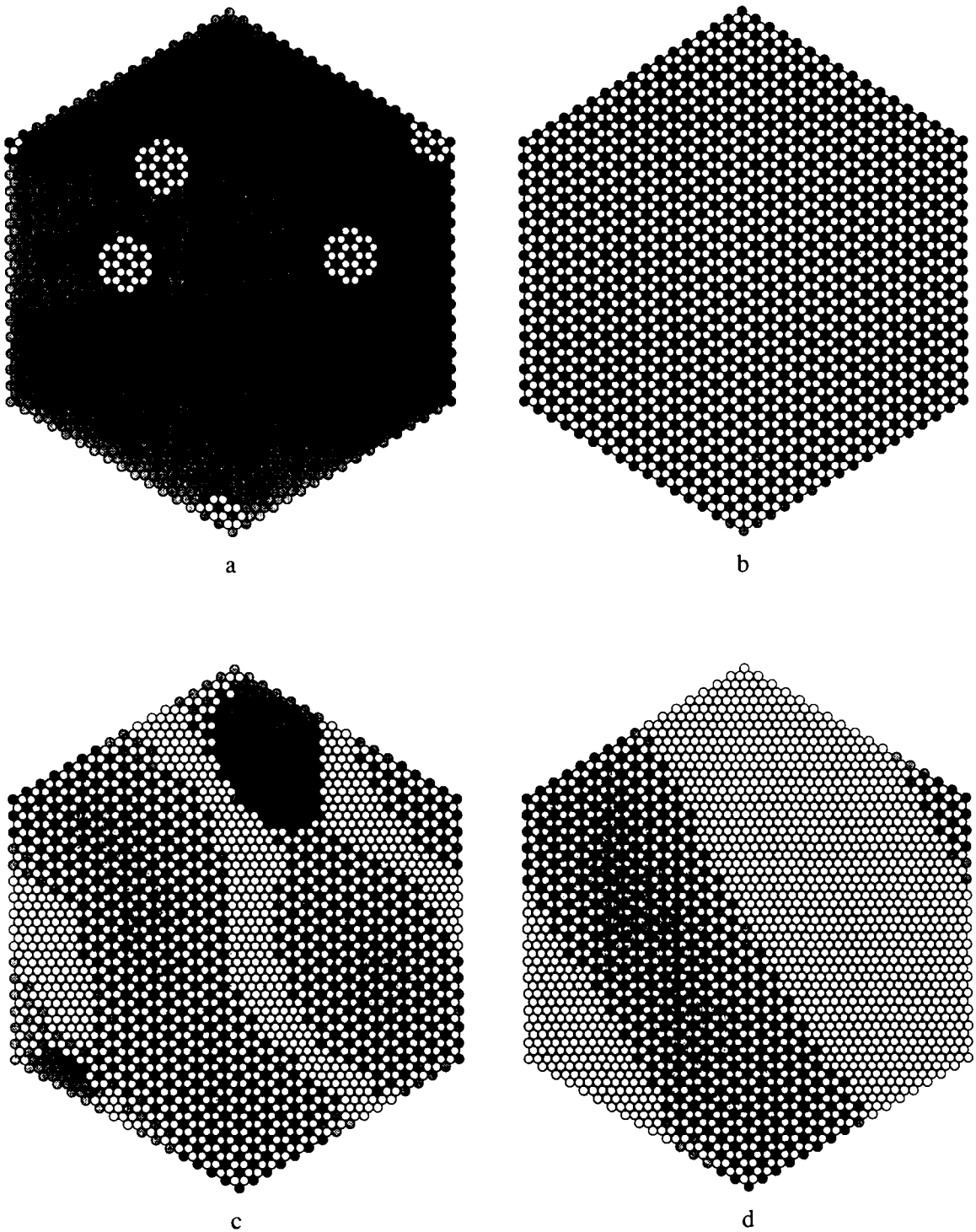
Fig. 10. Temporal evolution of occupation probabilities at lattice sites at composition 0.123 and temperature $T^* = 109$ in the ordering transition of first kind. Representation of the occupation probabilities is the same as Fig. 5. (a) $t^* = 0$; (b) $t^* = 18$; (c) $t^* = 100$; (d) $t^* = 500$.

mixture of the equilibrium ordered and disordered phases [Fig. 10(d)].

4.2.3. Composition $c = 0.103$. As is shown in Fig. 3, the representative point, a, of this system is within the two-phase field of the phase diagram but above the congruent equilibrium line. T_0 (at $T = T_0$, the free energies of the ordered and disordered phases are

equal). This area forms a very narrow strip adjacent to the solubility line for the disordered phase. According to thermodynamics, congruent ordering in this case is impossible. *The ordered phase can precipitate only by the classic mechanism through the nucleation and growth of the equilibrium ordered phase occurring with composition change.* Because of this we
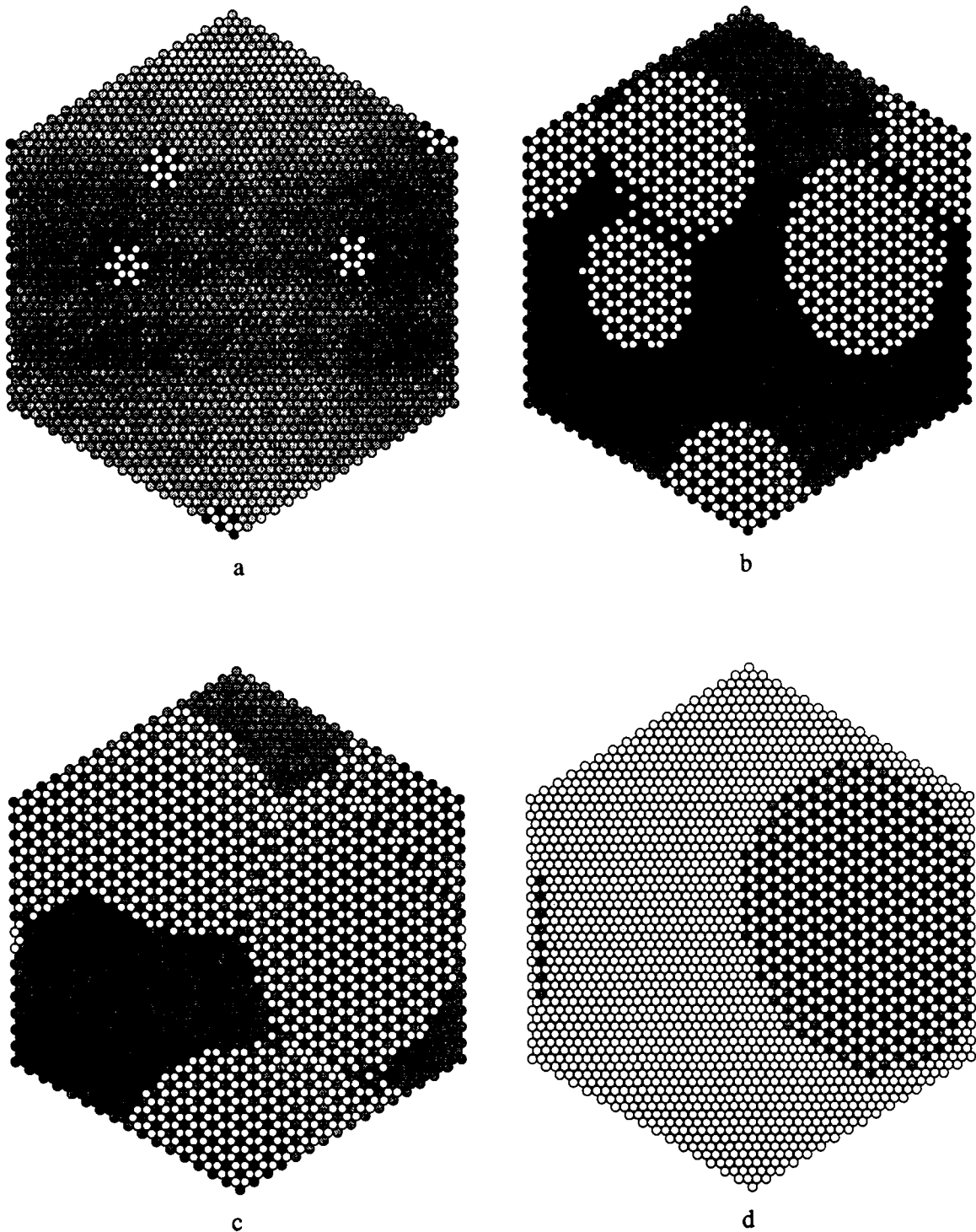
a

b

c

d

Fig. 11. Temporal evolution of occupation probabilities at lattice sites at composition 0.103 and temperature $T^* = 109$ in the ordering transition of the first kind. Representation of the occupation probabilities is the same as Fig. 5. (a) $t^* = 0$; (b) $t^* = 50$; (c) $t^* = 100$; (d) $t^* = 500$.

randomly placed four ordered phase nuclei with the radius $2a$ in the disordered matrix [Fix. 11(a)]. Unlike the previous case of $c = 0.123$, these nuclei were chosen so that they have the equilibrium composition and the equilibrium l.r.o. parameter of the ordered phase. The composition of the matrix is slightly

smaller than 0.103. However, the overall average composition is still maintained equal to 0.103.

Like in the $c = 0.123$ case, initial relaxation of the introduced nuclei results in the spreading of both, l.r.o. and composition profiles as shown in Fig. 11(b) corresponding to $t^* = 5$. The area of the ordered

region far exceeds the size of the nuclei. No congruent ordering throughout the system occures in this case. However, the order/disorder interface is very diffuse during decomposition. This suggests that congruent ordering occurs locally around the ordered phase nuclei. At $t^* = 100$, significant growth of the ordered phase has occurred and at the same time one of the ordered particles has disappeared due to coarsening [Fig. 11(c)]. The composition of the disordered matrix also moves towards the equilibrium composition at the same time. At $t^* = 1500$, both the decomposition and coarsening are almost completed [Fig. 11(d)]. The order/disorder interface compared to that at $t^* = 100$ is much shaper.

5. DISCUSSION

The method of kinetics equations for the density functions which are the averages over a time dependent nonequilibrium ensemble has a certain advantage with respect to the conventional Monte Carlo simulation. The Monte Carlo algorithm is designed to simulate the equilibrium Gibbs ensemble and produces a series of snapshot atomic configurations appearing along the simulated Markov chain. For our purposes, however, the determination of the temporal evolution of the single-particle characteristics such as local density and l.r.o. parameters described by the spatially inhomogeneous single-particle density function, $n(r)$, is of the primary concern. This is the reason why we used the kinetic equation method as a tool for the investigation of the relevant system. The accuracy of the free energy representation does not affect the main qualitative conclusions as long as the employed free energy gives qualitatively correct description of the convexity or concavity of the concentration and l.r.o. dependences of the free energy, and provides the correct topology of the phase diagram as shown in Fig. 1. The situation here is similar to that with the macroscopic phenomenological theory where the Landau free energy expansion can be successfully employed as long as it correctly describes the above-mentioned main topological features of the free energy dependence on composition and l.r.o. parameters.

The major limitation of our computer simulation technique is that it does not describe fluctuational nucleation and, this, cannot describe a transition from a metastable state. However, large fluctuations can be artificially introduced into the system in the form of random distribution of nuclei, as we have done for the compositions 0.123 and 0.103 for the ordering transition of the first kind.

In order to discuss the decomposition sequence of alloys in various regions of the phase diagram, we divide the two-phase field in Figs 2 and 3 into three regions, in which the free energy surfaces have different geometrical characteristics: the field (A) where $T < T(c)_- (c > c(T)_-)$, the field (B) where $T(c)_0 > T > T(c)_-$ $(c(T)_0 < c < c(T)_-)$ and the field

(C) where $T > T(c)_0$ $(c < c(T)_0)$. $T(c)_-$ is an absolute ordering instability temperature at composition c with respect to infinitesimal fluctuations of l.r.o. parameter, $T(c)_+$ is an absolute disordering instability temperature of the ordered phase at composition c and $T(c)_0$ is the congruent equilibrium temperature at which the free energies of the ordered and disordered phases at composition c are equal. The corresponding instability compositions $c(T)_-$, $c(T)_+$ and $c(T)_0$ are defined similarly. For the ordering transition of the second kind, $T(c)_0 = T(c)_-$, the two-phase field can be divided into two regions, below and above $T(c)_-$.

For any disordered alloy quenched to the field A or B, the free energy of the quenched disordered alloy is always higher than that of the ordered one at the same composition. The above situation is illustrated in Figs 4 and 8. Such a relation between the free energies of the ordered and disordered phases at the same composition makes the congruent ordering always possible. Depending on the temperature of aging, the ordering should occur either by nucleation of the ordered phase domains of the same composition (in field B), or by the barrierless homogeneous ordering (in field A). But in both cases the resultant state is the same. It is the single phase transient ordered phase.

In the area (C) the thermodynamics forbids the congruent ordering at all since the free energy of the ordered phase is never below the free energy of the disordered phase at the same composition (see Fig. 8 at $c < c_0$). Therefore the decompositon in the area (C) can occur only by the conventional mechanism, i.e. by the precipitation of equilibrium ordered phase particles from the disordered matrix. The area (C) where the conventional precipitation mechanism occurs is very narrow compared to the whole two-phase field.

In our computer simulation of the decomposition with the ordering transition of the second kind all compositions of the disordered alloys, $c = 0.15, 0.25,$ 0.415, were chosen so that the aging occurred in the area (A). Figures 5(a), 6(a), 7(a) demonstrate that for all these alloys the decomposition reaction starts from the congruent ordering which produced the transient nonstoichiometric ordered single-phase state.

For the ordering transition of the first kind, we chose the alloy with $c = 0.165$ in the area (A) (point c in Fig. 3), the alloy with $c = 0.123$ in the area (B) (point b) and the alloy with $c = 0.103$ in the area (C) (point a). The computer simulation shows that the alloy with $c = 0.165$ decomposition started from barrierless congruent ordering resulting in the ordered single-phase state [Fig. 9(a–d)] in agreement with the thermodynamic analysis. The decay of the l.r.o. fluctuations observed in the computer simulation of the alloy with $c = 0.123$ is also consistent with the thermodynamics since an alloy in the area (B) should be stable with respect to small fluctuations

of the l.r.o. parameter, η. We have shown, however, that the artificially introduced ordered nuclei whose size is above the critical one can grow congruently, producing a single-phase ordered phase prior to the decomposition (Fig. 10). The simulation for the alloy with $c = 0.103$ located in the area (C) where the congruent ordering is impossible shows that the alloy decomposes only if the critical nuclei of the equilibrium ordered phase are introduced. The decomposition occurs by the growth of the equilibrium phase followed by the coarsening [Figs 11(a–d)]. It is very interesting that even in this case where the thermodynamics predicts the conventional decomposition mechanism, the mechanism which follows from our computer simulation has features different from what we would have expected. As follows from Fig. 11(b, c), the growth occurs in two stages by a very unconventional way. The first stage is congruent ordering around the ordered phase nuclei, the area of the congruent ordering substantially exceeding the area occupied by the nuclei, and the second stage is the subsequent decomposition of these congruently ordered regions. The coarsening mechanism, however, is the same as that is predicted by the conventional theory.

The transient ordered states formed due to the congruent ordering undergo either the isostructural spinodal decomposition into two ordered phases (if the alloy is quenched below the conditional spinodal as has been proposed by Allen and Cahn for the ordering of the second kind [6]) or by nucleation of the equilibrium disordered phase. Figure 10 illustrates that the spinodal decomposition occurs by a separation of the initial congruently ordered phase into two ordered phases with the same structure but different compositions. The composition of the solute-lean phase moves towards the solubility line of the disordered α phase of the phase diagram (see Fig. 3). It spontaneously disorders when it reaches the instability line, $T(c)_+$, above which the ordered phase is unstable [1]. The composition of the solute-rich ordered phase moves during this spinodal decomposition in the opposite direction towards the solubility line of the ordered β phase up to the moment when it reaches its equilibrium composition, c_β, producing the β phase. Figure 10 of our computer simulation results confirms this cascade of decomposition reactions predicted in [1] on the basis of thermodynamics. It should be, however, emphasized that substantial homogeneous decomposition can be observed only within very large domains of the congruently ordered phase (Figs 6 and 10). Some decomposition is also observed inside the relatively large domains of Figs 5 and 9 but no completely disordered phase develops.

Our computer simulation predicts that the precipitation of the ordered intermetallics through a single-phase nonstoichiometric ordered state substantially alters the decomposition mechanism even with respect to what could be expected from the

thermodynamic analysis [1] and [5]. The computer simulation revealed a crucial role played by the APBs formed in the single-phase ordered state in the decomposition kinetics. As it follows from Figs 5, 7 and 9, the decomposition mainly occurs heterogeneously at the APBs, regardless if the alloy is inside or outside the conditional spinodal. This decomposition replaces the APBs by a layer of the equilibrium disordered phase enveloping the ordered phase domains and, thus, creating a very specific "shell" structure [Figs 5(a), 7(b) and 9(b)]. The electron microscopic observation of "speckles" of the ordered phase domains in Al–Li alloy aged at low temperatures by Sato et al. [2] is probably related to the fine scale "shell" structure stage of the decomposition kinetics.

The dominant decomposition at the APBs resulting in their wetting by the disordered phase is a manifestation of a special kind of instability which is more effective than the conventional spinodal instability within the domains. The latter is just a minor process which, in most cases, does not contribute too much to the overall decomposition rate. The nature of the APB instability could be, for example, clarified by a limit transition to the continuum equations by expanding the microscopic kinetic equations (2) or (4) around $\mathbf{k} = 0$ and $\mathbf{k} = \mathbf{k}_0$. The expansion around $\mathbf{k} = 0$ gives the continuum kinetic equation for composition while the expansion around $\mathbf{k} = \mathbf{k}_0$ results in the continuum kinetic equation for the l.r.o. parameter. In the real space these continuum counterparts of (2) and (4) read

$$\frac{\partial c}{\partial t} = D\left[-m_c \nabla^4 c + \nabla^2 \frac{\partial f(c, \eta)}{\partial c} \right] \quad (19)$$

$$\frac{\partial \eta}{\partial t} = -L_\eta \left[-m_\eta \nabla^2 \eta + \frac{\partial f(c, \eta)}{\partial \eta} \right] \quad (20)$$

where $f(c, \eta)$ is the local free energy per unit volume, and m_c and m_η are gradient coefficients for the composition and l.r.o. parameter, respectively. Within the antiphase domains where the congruently ordered phase is homogeneous [$c(\mathbf{r}) =$ const. and $\eta(\mathbf{r}) =$ const.], equation (19) does not give any decomposition since $\partial c/\partial t = 0$. This means that the spinodal decomposition of the completely homogeneous ordered solution cannot occur within Cahn's approximation (19) even if the alloy is below the conditional spinodal (the spinodal decomposition would, of course, appear in the next approximation which takes into account the simultaneous temporal evolution of the two-particle correlation function). This conclusion shows that the spinodal decomposition within the transient phase ordered domains where $c(\mathbf{r}) \approx$ const and $\eta(\mathbf{r}) \approx$ const. does not occur at all or occurs very slowly. At the APBs, however, where, by its definition, $\eta = \eta(\mathbf{r})$, the right-hand side of equation (19) does not vanish since $\partial f(c, \eta)/\partial c$ depends on the coordinates through $\eta(\mathbf{r})$. Therefore, the decompositon rate, $\partial c/\partial t$, does not vanish and the

barrierless temporal concentration evolution at the APBs resulting in the decomposition should occur even at the first approximation (19). This results in the conclusion that the above discussed concentrational instability at the APBs is induced by the inhomogeneity of the l.r.o. of the ordered phase in the form of APBs.

Actually the instability resulting in APBs wetted by a disordered phase has been first discussed by Allen and Cahn based on experimental observations in the Fe–Al system [6]. Matsmura et al. [16] analyzed the kinetics of segregation of solvent atoms into the APB using a simple Landau-type free energy expansion for the ordering transition of the second kind, equation (19), and assuming a one-dimensional square distribution of l.r.o. parameter in the ordered phase. They also concluded that the segregation of the solvent atoms into the APB is barrierless and therefore is a kind of spinodal instability.

The final microstructure is developed due to the coarsening which, according to our computer simulation, results in formation of the ultimate equilibrium two-phase system dictated by the phase diagrams. Our computer simulation shows that there are two types of coarsening. The first one is a coarsening of anitphase domains in the single-phase congruently ordered state. It is driven by the reduction of APB surface area. The second is the conventional coarsening developed after the decomposition of the ordered single-phase state. It is driven by the reduction of the order/disorder interfacial area.

In most situations, coarsening is driven by reduction in the order/disorder interfacial energy since a disordered film develops soon after the formation of the congruent ordered phase, e.g. in the cases of composition $c = 0.15$, $c = 0.25$ and $c = 0.415$ in the ordering transition of the second kind and $c = 0.165$ in the ordering transition of the first kind. Coarsening proceeds by both a surface diffusion along the order/disorder interface and bulk diffusion across the ordered and disordered phases.

Coarsening of antiphase domains driven by the APB energy reduction occurs in the case of $c = 0.15$ during ordering stage in the ordering transition of the second kind and $c = 0.123$ during congruent growth stage in the ordering transition of the first kind. These two compositions are quite close to the T_0 line and therefore, the driving force for ordering is small compared to other compositions. It takes longer time to reach the congruent ordered state than other compositions studied in this paper. Moreover, the order/disorder interface is very diffuse close to T_0 line, hence different ordered domains interact during growth which leads to coarsening.

In summary, the decomposition of a disordered phase quenched into a two-phase field of ordered and disordered phase occurs, as a rule, in three stages even though they sometimes overlap each other. The first stage is a congruent ordering reaction which produces an ordered single-phase alloy composed of antiphase domains. The second stage is the decomposition of the congruently ordered state, which predominantly occurs along the APBs. And the last stage is the coarsening of the decomposed two-phase mixture, which is driven by the reduction of the total order/disorder interfacial energy. The only exception to this sequence of transformation is when the alloy composition is inside the field C which is a very small region compared to the overall two-phase field.

The predictions obtained in this computer simulation study are confirmed by Allen and Cahn for Fe–Al alloys [6], Matsumura et al. for Fe–Si alloys [16], Sato et al [2], Radmilovich et al. [3] and Shaiu et al. [4] for Al–Li alloys, and by Corey and Lisowski [17] and Corey et al. [18] for Ni–Al superalloys.

In the initial stage of decomposition at room temperature Sato et al. observed extremely fine domains of the ordered intermetallic Al_3Li phase separated by the boundary areas with incompletely ordered structure which later developed in the normal two-phase structure [2]. Similar effects were observed by Radmilovich et al. [3]. They reported the l.r.o. parameter to be around 0.5 of the normal one which is consistent with the fact that the observed state is a congruently ordered one. Shaiu et al. reported that the composition along the sample with the ordered domains is constant which is in agreement with the concept of the congruent ordering. They also concluded that the congruent ordering occurs prior to the decomposition. The boundaries between domains observed in [2, 3] seem to be APBs which has a structure similar to that obtained in our computer simulation [see for example, Figs 5(b), 6(b), 7(b) and 9(b)]. As is shown above, the decomposition on these boundaries is associated with the specific APB concentration instability competing with the conventional spinodal instability.

Although the decomposition kinetics in superalloys is one of the best studied processes, the formation of the congruent ordered state at the initial stage has been largely overlooked. To our knowledge, the papers which address this phenomenon are the single crystal X-ray study by Corey and Lisowski [17], and transmission electron microscopy study by Corey et al. [18]. These researchers gave the most clear indication that the congruent ordering precedes the decomposition process in Ni–Al alloy. They observed the formation of a transient single–phase state (they called it the γ^* phase) prior to the precipitation of the Ni_3Al phase. The γ^* phase has the same ordered structure as the equilibrium Ni_3Al phase but its composition is different. It actually coincides with the as quenched composition of the disordered phase, which is within the two-phase field of the diagram. According to our computer simulation results and general thermodynamic analysis [1, 5] the similar sequence of the structural transformations during the precipitation of the ordered intermetallic phase should be expected in all systems.

We believe that the congruent ordering may even produce the transient ordered phases whose structures are different from those of the stable phases on the phase diagram. It could be, in principle, expected in systems like Cu–Al within the $\alpha(Cu) + \beta(CuAl)$ area. In Cu–Al system a congruently ordered f.c.c.-based transient phase is predicted if the interactions between Cu and Al atoms in the f.c.c. solution is such that each Cu atom tries to have Al atoms as the nearest-neighbors. The structure of the congruently ordered phase then would be determined by details of the interchange interaction.

The same phenomenon can be expected in ceramic compounds with mixed valencies (this condition is required to allow deviations from the stoichiometry). The transient single phase state then could be formed either by congruent ordering or by diffusionless displacive transformation. In this respect it should be mentioned that the ordering considered above is not the only possible congruent reaction which may precede the decomposition. The martensitic transformation is another possibility. It appears when the structural parameter distinguishing the parent and product phase is an amplitude of a crystal lattice rearrangement mode.

The above obtained conclusions concerning the transformation path during the precipitation of a ordered intermetallic phase can be extended to precipitation of a secondary ordered phase from the primary ordered phase matrix. This case is expected in the systems characterized by two l.r.o. parameters. An exmaple of such a decomposition is discussed by Matsumura et al. [16] who studied the decomposition of the B2 primary ordered phase in Fe–Si alloys into a mixture of the B2 phase and the secondary ordered DO_3 (Fe_3Si) phase. If a disordered alloy is quenched into the two-phase field, then two congruent ordering reactions, primary and secondary, should occur prior to the decomposition. This would produce the transient single-phase ordered state with two types of the antiphase domains and, thus, two types of APBs which will create different instabilities with respect to the further decomposition. In this case many different structural transformation paths depending on the position of the representative point in the phase diagram are possible.

The precipitation mechanism involving the congruent ordering is very important since this phenomenon can be expected in the majority of advanced structural alloys. Typical examples of such alloys are discussed above. They are the family of Ni-based superalloys, Al–Li, Fe–Al, Al–Ti and other similar materials. Since the "shell" structure predicted by the present computer simulation may considerably affect the mechanical and other properties of the alloy, it could be, for example, used for the alloy design. In particular, it has been shown that the "shell" structure enhances the ductility of Ni–Al superalloys considerably [19]. The "shell" structure is formed by layers of the disordered phase encircling the ordered

phase particles which substitute the APBs. Thus the configuration of the order/disorder interfacial boundaries coincides with the APB network at the initial stage of the decomposition of the congruently ordered state. Therefore, controlling the size and distribution of the antiphase domains at the stage of the congruent ordering, we can, up to a certain extent, control the structure of the two-phase mixture.

6. CONCLUSION

In this paper we have conducted a computer simulation study which describes ordering, decomposition and coarsening simultaneously. The main conclusion is that the precipitation of an ordered intermetallic phase from a disordered phase, in general, does not occur by the conventional nucleation and growth mechanism. In most parts of the phase diagram, the precipitation occurs in three stages. At the first stage, a transient nonstoichiometric phase which has the same composition as the original disordered solid solution and the same symmetry as the final ordered phase is formed by the congruent ordering reaction. In the case of ordering transition of the first kind, the transient ordered phase can either arise from the ordering instability or nucleation and growth. The next stage is the decomposition of the transient ordered phase. It occurs prediminantly at the APBs. This is true even the composition is inside the conditional spinodal of the ordered phase, where the ordered phase can spinodally decompose. Decomposition at APBs is due to a concentrational instability induced by the inhomogeneities in the l.r.o. of the congruently ordered phase. The last stage is coarsening process of the decomposed two-phase microstructure, which is slower than both the ordering and decomposition rection. The preceding wetting of the APBs by a disordered film can slow the coarsening process of the ordered phase substantially, which may be utilized for formation of very fine two-phase mixtures. The only exception to the above-described transformation sequence is for alloy compositions between the solvus line of the disordered phase and the T_0 line, which is a very narrow strip in the equilibrium phase diagram.

REFERENCES

1. A. G. Khachaturyan, T. F. Lindsey and J. W. Morris Jr, *Metall. Trans.* **19A**, 249 (1988).
2. T. Sato, N. Tanaka and T. Takahashi, *Trans. Japan Inst. Metals* **29**, 17 (1988).
3. M. Radmilovich, A. G. Fox and G. Thomas, *Acta metall.* **37**, 2385 (1989).
4. B.-J. Shaiu, H.-T. Li and Haydn Chen, in *Proc. Fifth Int. Conf. on Al–Li*, Williamsburgh, Pa (1989).

5. W. A. Soffa and D. E. Laughlin, *Acta metall.* **37**, 3019 (1989).
6. S. M. Allen and J. W. Cahn, *Acta metall.* **24**, 425 (1976).
7. W. A. Soffa and D. E. Laughlin, *Solid–Solid Phase Transformations* (edited by M. Aaronson, D. E. Laughlin and C. M. Wayman), p. 159. T.M.S.-A.I.M.E., Warrendale, Pa (1981).
8. S. V. Semenovskaya, *Physica status solidi* (b) **64**, 291 (1974).
9. H. Kubo and C. M. Wayman, *Acta metall.* **28**, 398 (1980).
10. A. G. Khachaturyan, *Soviet Phys. Solid St.* **9**, 2040 (1968).
11. A. G. Khachaturyan, *Theory of Structural Transformations in Solids.* Wiley, New York (1983).
12. J. W. Cahn and J. E. Hilliard, *J. chem. Phys.* **28**, 258 (1958).
13. V. G. Vaks, A. J. Larkin and C. A. Pikin, *Zh. Eks. Teor. Fiz. (JETP)* **51**, 361 (1966) (in Russian).
14. A. G. Khachaturyan, *Phys. Met. Metallogr.* **13**, 493, (1962); *Soviet Phys. Solid St.* **5**, 548, (1963); *Physica status solidi* (b) **60**, 19 (1973).
15. P. R. Swann, W. R. Duff and R. M. Fisher, *Metall. Trans.* **3**, 409 (1972).
16. S. Matsumura, H. Oyama and K. Oki, *Mater. Trans., Japan Inst. Metals* **30**, 695 (1989).
17. C. L. Corey and B. Lisowski, *Trans. metall. Soc. A.I.M.E.*, **239**, 239 (1967).
18. C. L. Corey, B. Z. Rosenblum and G. M. Greene, *Acta metall.* **21**, 837 (1973).
19. R. W. Cahn, *High-Temperature Ordered Intermetallic Alloys—II* (edited by N. S. Stoloff, C. C. Koch, C. T. Liu and O. Izumi), Vol. 81, p. 27, MRS Proc. (1987).